The Novel Secreted Factor MIG-18 Acts with MIG-17/ADAMTS to Control Cell Migration in *Caenorhabditis elegans*

Hon-Song Kim,* Yuko Kitano,†,‡ Masataka Mori,* Tomomi Takano,* Thomas Edward Harbaugh,§ Kae Mizutani,* Haruka Yanagimoto,* Sayaka Miwa,* Shinji Ihara,† Yukihiko Kubota,*, Yukimasa Shibata,* Kohji Ikenishi,‡ Gian Garriga,§ and Kiyoji Nishiwaki*,†,1**

*Department of Bioscience, Kwansei Gakuin University, Sanda 669-1337, Japan, †RIKEN Center for Developmental Biology, Chuo-ku, Kobe 650-0047, Japan, ‡Department of Biology, Graduate School of Science, Osaka City University, Sugimoto, Sumiyoshi, Osaka 558-8585, Japan, §Department of Molecular and Cell Biology, University of California, Berkeley, Calfornia 94720, and **Department of Developmental Biology and Neurosciences, Graduate School of Life Sciences, Tohoku University, Aoba-ku, Sendai 980-8577, Japan

ABSTRACT The migration of *Caenorhabditis elegans* gonadal distal tip cells (DTCs) offers an excellent model to study the migration of epithelial tubes in organogenesis. *mig-18* mutants cause meandering or wandering migration of DTCs during gonad formation, which is very similar to that observed in animals with mutations in *mig-17*, which encodes a secreted metalloprotease of the ADAMTS (**a** **d**isintegrin **a**nd **m**etalloprotease with **t**hrombo**s**pondin motifs) family. MIG-18 is a novel secreted protein that is conserved only among nematode species. The *mig-17(null)* and *mig-18* double mutants exhibited phenotypes similar to those in *mig-17(null)* single mutants. In addition, the mutations in *fbl-1/fibulin-1* and *let-2/collagen IV* that suppress *mig-17* mutations also suppressed the *mig-18* mutation, suggesting that *mig-18* and *mig-17* function in a common genetic pathway. The Venus-MIG-18 fusion protein was secreted from muscle cells and localized to the gonadal basement membrane, a tissue distribution reminiscent of that observed for MIG-17. Overexpression of MIG-18 in *mig-17* mutants and vice versa partially rescued the relevant DTC migration defects, suggesting that MIG-18 and MIG-17 act cooperatively rather than sequentially. We propose that MIG-18 may be a cofactor of MIG-17/ADAMTS that functions in the regulation of the gonadal basement membrane to achieve proper direction of DTC migration during gonadogenesis.

THE ADAMTS (**a** **d**isintegrin **a**nd **m**etalloprotease with **t**hrombo**s**pondin motifs) family of the secreted zinc metalloproteases has important roles in development. Nineteen ADAMTS genes have been identified in the human genome, and mutations in many result in hereditary diseases that are related to disorders of the extracellular matrix (Apte 2009). The functions of ADAMTS-5, -9, and -20 are required for digit formation, and ADAMTS-9 and -20 are needed for closure of the palate in mice (McCulloch *et al.* 2009; Enomoto *et al.* 2010). ADAMTS-5 and -15 act in myoblast fusion (Stupka *et al.* 2013). However, the precise roles of ADAMTS proteases in development still remain elusive.

Among five ADAMTS genes in *Caenorhabditis elegans*, *gon-1* and *mig-17* play essential roles in the development of the somatic gonad (Blelloch and Kimble 1999; Nishiwaki *et al.* 2000). GON-1 is required for active migration of gonadal distal tip cells (DTCs), whereas MIG-17 acts in the directional control of DTC migration. Genetic suppressor analyses of *mig-17* mutants identified dominant gain-of-function (*gf*) mutations in two genes that encode basement membrane proteins, FBL-1C/fibulin-1C and LET-2/α2 subunit of collagen IV (Kubota *et al.* 2004, 2008). The suppressor *fbl-1(gf)* mutations result in substitutions of evolutionarily conserved amino acids within the second EGF-like motif of FBL-1C. FBL-1C is recruited to the gonadal basement membrane by MIG-17 activity, where it is likely to be required for directional control of DTC migration (Kubota *et al.* 2004). The suppression by *fbl-1(gf)* mutations depends on NID-1/nidogen, a basement membrane protein

doi: 10.1534/genetics.113.157685
Manuscript received September 19, 2013; accepted for publication November 24, 2013; published Early Online December 6, 2013.
Supporting information is available online at http://www.genetics.org/lookup/suppl/doi:10.1534/genetics.113.157685/-/DC1.
[1]Corresponding author: Department of Bioscience, Kwansei Gakuin University, 2-1 Gakuen, Sanda 669-1337, Japan. E-mail: nishiwaki@kwansei.ac.jp

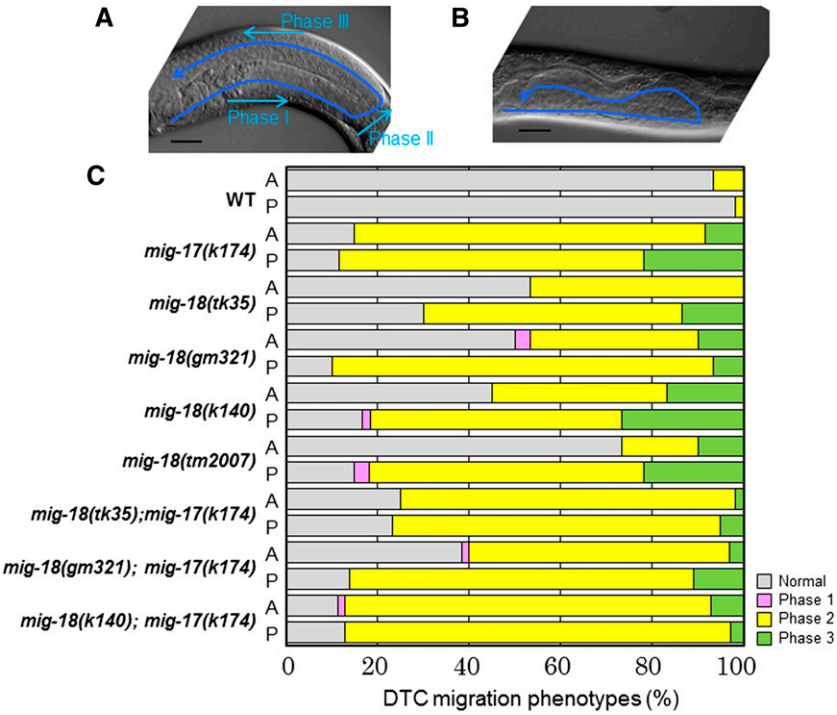

Figure 1 Defective DTC migration of *mig-18* mutants. (A and B) Gonad morphology (arrows) of wild-type (A) and *mig-18(k140)* (B) young-adult hermaphrodites. Posterior gonads are shown. Anterior to the left, dorsal to the top. Bar, 20 μm. The phases of DTC migration are indicated. Both phase II and phase III are defective in B. (C) Percentages of abnormal gonad morphology in the *mig-18* and *mig-18*; *mig-17* double mutants. The DTC migration defects were scored based on the earliest defective phase. $n = 60$ for each experiment.

(Kubota *et al.* 2008). The two suppressor *let-2(gf)* mutations result in amino acid changes in the triple helix region and in the C-terminal noncollagenous domain. In contrast to *fbl-1(gf)* mutations, suppression by *let-2(gf)* mutations is NID-1 independent (Kubota *et al.* 2008).

In this study, we analyzed a novel gene, *mig-18*, mutations in which led to misdirected migration of DTCs similar to that observed in *mig-17* mutants. *mig-18* was found to encode a small protein that was secreted from muscle cells and localized to the gonadal basement membrane. This tissue distribution of MIG-18 was similar to that observed for MIG-17. The phenotypic analysis of *mig-18*; *mig-17* double mutants revealed that *mig-18* did not enhance the phenotype of the *mig-17* null allele. Furthermore, *fbl-1(gf)* and *let-2(gf)* mutations that suppressed *mig-17* also suppressed the DTC migration defects in the *mig-18* mutants. These results suggest that MIG-18 acts in the same pathway with MIG-17. Genetic and molecular evidence suggests that MIG-18 functions together with MIG-17/ADAMTS to control directional migration of DTCs.

Materials and Methods

Strains and genetic analysis

Culture, handling, and ethyl methanesulfonate (EMS) mutagenesis of *C. elegans* were conducted as described (Brenner 1974). The following mutations were used in this work: *mig-18(k140)*, *fbl-1(k201*, *k206)*, *let-2(k196)*, *nid-1(cg118*, *cg119)*, *unc-25(e156)*, *unc-42(e270)*, *unc-64(e246)*, and *unc-119(e2498)* (Brenner 1974; Maduro and Pilgrim 1995; Nishiwaki 1999). *mig-18(gm321)* and *mig-18(tk35)* were isolated by genetic screening using EMS and *N*-ethyl-*N*-nitrosourea as mutagens, respectively (Brenner 1974; De Stasio and Dorman 2001). *mig-18(tm2007)* was obtained from the National Bioresource Project for the nematode. The transgenic extrachromosomal arrays containing *nid-1*::*HA* (Kubota *et al.* 2008) were introduced into *mig-18(k140)*-containing strains by mating.

Microscopy

Gonad migration phenotypes were scored using a Nomarski microscope (Axioplan 2; Zeiss). Analysis of gonadal phenotypes was performed at the young-adult stage as described (Nishiwaki 1999). The patterns of expression of Venus fusion proteins (see below) were analyzed using a confocal laser-scanning microscope (LSM5; Zeiss) equipped with a C-Apochromat 63× (water immersion; numerical aperture 1.2) lens and controlled by PASCAL version 3.2 SP2 software.

Molecular cloning of mig-18

mig-18 was mapped to the right of *unc-64* on linkage group III. Single-nucleotide polymorphism mapping (Wicks *et al.* 2001) placed it to the right of the cosmid clone T03F6. Microinjection rescue experiments using 12 fosmid clones that covered most of the region between T03F6 and the right end of the chromosome identified a fosmid clone, WRM0613bA03, that rescued the *mig-18* DTC migration defects. A PCR-amplified fragment of one of the predicted genes contained within this fosmid clone, *F11F1.6*, rescued *mig-18*. Genomic sequence analyses revealed nucleotide changes in the coding regions of *F11F1.6* in all three mutant alleles of *mig-18*.

Constructs

To construct *mig-18p*::*SP*::*Venus*::*mig-18*, the genomic region of *mig-18* from −921 to +2022, relative to the adenine of the

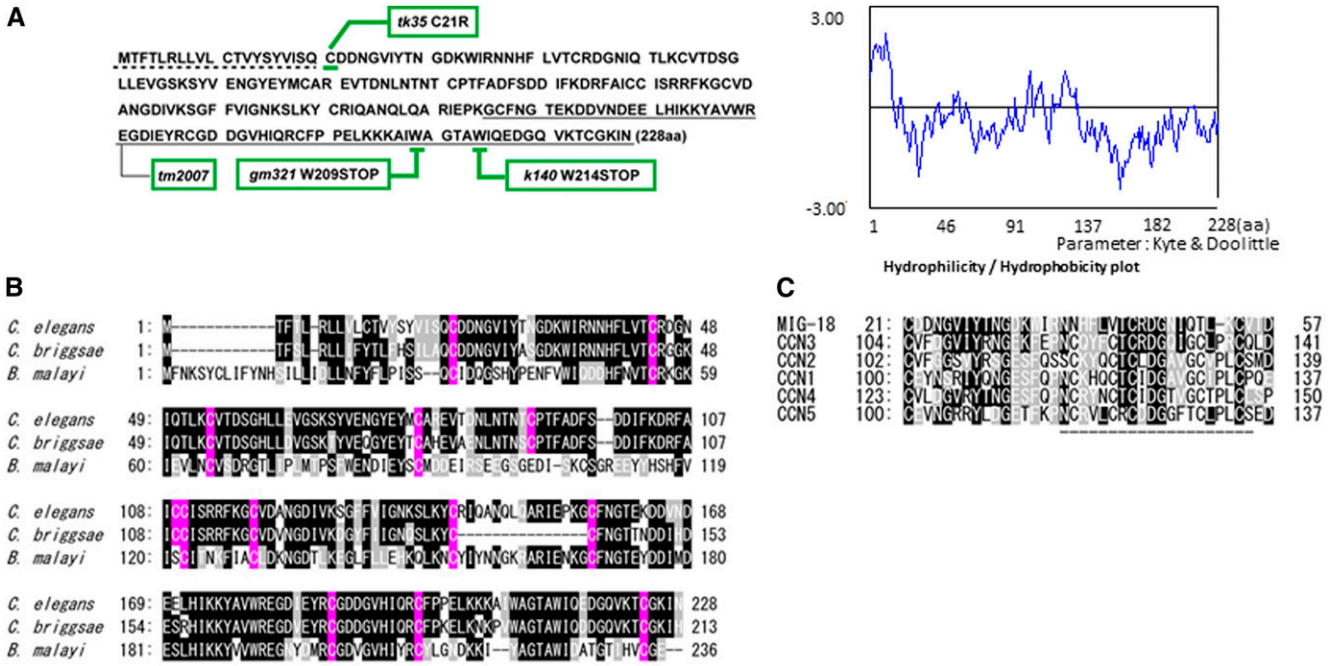

Figure 2 MIG-18 and its homologs. (A) Amino acid sequence of MIG-18 (left) and hydrophilicity/hydrophobicity plot (right). Positions of *mig-18* mutations are indicated. Nucleotide changes are *tk35*, C21R (tgt > cgt); *gm321*, W209STOP (tgg > tga); and *k140*, W214STOP (tgg > tag). *tm2007* potentially truncates the underlined amino acids due to the 472-bp deletion from g571 with respect to the adenine of the initiation codon, which is within the second intron. The dotted line (left) indicates the potential signal peptide. (B) MIG-18 homologs in nematodes. *C. elegans*, MIG-18; *Caenorhabditis briggsae*, CBG21220; *Brugia malayi*, Bm1_50515. Identical and similar amino acids are shown by black and gray boxes, respectively. Cysteine residues are shown in pink. (C) Homologous regions between MIG-18 and mouse CCN family proteins. Identical and similar amino acids are shown by black and gray boxes, respectively. The region indicated by the dashed line corresponds to the integrin-binding site in human CCN1 (Chen *et al.* 2004). Analysis of amino acid sequences was done using GENETYX Version 8.

initiation codon, was amplified by PCR and was cloned into pBluescriptII KS(−) (Invitrogen). The plasmid carrying the *Venus* gene was kindly provided by Takeshi Ishihara. The *Venus* gene was amplified by PCR and was inserted downstream of the signal peptide sequence (+69) of *mig-18*. To remove the signal peptide sequence, the plasmid *mig-18p*::*SP*::*Venus*::*mig-18*, except for the signal peptide sequence, was amplified by PCR and was self-ligated, producing *mig-18p*::*ΔSP*::*Venus*::*mig-18*. To construct *mig-24p*::*TM*::*Venus*::*mig-18*, the *SP* sequence of *mig-18p*::*SP*::*Venus*::*mig-18* plasmid was replaced with the genomic region of *mig-22*, from +1 to +195 in exon 1, which encodes the type II transmembrane (TM) domain (Suzuki *et al.* 2006). To construct *mig-17p*::*mig-17*::*Venus* and *mig-17p*::*mig-17*::*mCherry*, the *GFP*-coding sequence of the *mig-17p*::*mig-17*::*GFP* plasmid (Nishiwaki *et al.* 2000) was replaced with those of *Venus* and *mCherry* from pPD95.79, respectively.

Germline transformation

Germline transformation was carried out as described (Mello *et al.* 1991). Transgenic strains were made by injecting plasmids into *unc-119(e2498)* hermaphrodites, and the generated transgenic arrays were transferred to appropriate genetic backgrounds having *unc-119(e2498)* by mating. *mig-18p*::*SP*::*Venus*::*mig-18* plasmid was injected at 5 ng/μl with 25 ng/μl *unc-119*$^{+}$ plasmid (pDP#MM016B) (Maduro and Pilgrim 1995) and 100 ng/μl pBluescriptII KS(–) (carrier DNA). *mig-24p*::*mig-22TM*::*Venus*::*mig-18* plasmid was injected at 10 ng/μl with 30 ng/μl pDP#MM016B and 130 ng/μl pBluescriptII KS(–). *mig-17p*::*mig-17*::*Venus* plasmid was injected at 100 ng/μl with 25 ng/μl pDP#MM016B and 25 ng/μl pBluescriptII KS(–).

Western blot analysis

Western blot analysis was done as described (Ihara and Nishiwaki 2007).

Quantification of FBL-1C localization

The method for quantification of FBL-1C localization to the basement membrane is shown in supporting information, Figure S1.

Results

mig-18 encodes a novel secreted protein required for directional migration of the DTCs

The *C. elegans* gonad arms extend to the anterior-right and posterior-left areas of the body cavity. The U-shape of the gonad arms reflects the migration paths of the gonadal DTCs during larval development (Figure 1A). The DTCs are generated at the tip of the gonad primordium and migrate in opposite directions along the ventral body-wall muscle (phase I).

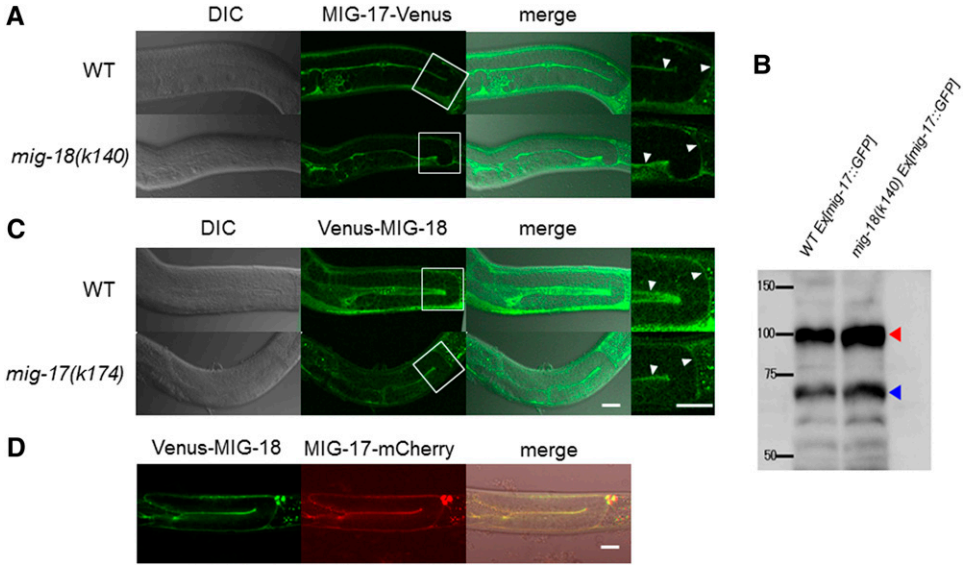

Figure 3 Expression and localization of MIG-17-Venus and Venus-MIG-18. (A and C) DIC (left), confocal (center), and merged (right) images. The enlarged images of the boxed areas in the center panels are shown on the right side. The arrowheads point to the fluorescence from the gonadal basement membrane. (A) Wild-type and *mig-18(k140)* young adults that express MIG-17-Venus. (B) Western blot analysis of wild-type and *mig-18(k140)* animals that expressed MIG-17-GFP. Worm extracts (200 μg protein/sample) were analyzed using rabbit anti-GFP (2 mg/ml, Molecular Probes). The red and blue arrowheads indicate pro- and mature forms MIG-17-GFP, respectively. Intensities of the bands were quantified using ImageJ software. (C) Venus-MIG-18 expression in wild-type and *mig-17(k174)* animals. (D) Colocalization of Venus-MIG-18 and MIG-17-mCherry in the gonadal basement membrane. Confocal images for Venus (left) and mCherry (center) and DIC and confocal merged image (right). The strong dot-like signals on the upper right are of coelomocytes that take up secreted proteins. Posterior gonads are shown. Anterior to the left, dorsal to the top. Bar, 20 μm.

They turn dorsally and migrate over the lateral hypodermis toward the dorsal body-wall muscle (phase II). Upon reaching the dorsal muscle, the two DTCs turn again and migrate toward the midbody along the dorsal muscle (phase III) (Hedgecock *et al.* 1987). We isolated three independent mutants in the *mig-18* gene by forward genetics screening of gonad morphology. The *mig-18* mutants showed defects in phase II and phase III migration, but the phase I migration was essentially normal (Figure 1B). In the mutant animals, the DTCs often partially executed the dorsal migration and moved over the lateral hypodermis, rather than the dorsal muscle, after the second turn (Figure 1, B and C).

We cloned *mig-18* by genetic mapping followed by injection rescue experiments using genomic DNA fragments (data not shown). *mig-18* corresponded to the predicted gene *F11F1.6* in WormBase. The predicted MIG-18 protein, which consists of 228 amino acids, apparently has homologs only in nematodes (Figure 2, A and B). MIG-18 appeared to be a secreted protein because it has a potential signal peptide for secretion at its N terminus and cysteine motifs that are well conserved among nematode species. Although we could not find orthologs of MIG-18 in other species, we identified a 37-amino-acid stretch that has considerable homologies with the CCN [**C**yr61 (cysteine-rich protein 61), **C**TGF (connective tissue growth factor), and **N**OV (nephroblastoma overexpressed gene)] family of secreted proteins in mammals (Chen and Lau 2009). Among the CCN proteins, MIG-18 was most similar to CCN3 (Figure 2C). This homologous region contains a 20-amino-acid sequence identified as the binding site for integrin αvβ3 in CCN1 (Chen *et al.* 2004), although some cysteine residues were not conserved in MIG-18.

The mutations *k140* and *gm321* were nonsense mutations that occurred near the C terminus of the gene, whereas *tk35* was an amino acid substitution of the cysteine immediately after the signal peptide. *tm2007* was a deletion mutation that may truncate the C-terminal 73 amino acids (Figure 2A). The *k140* and *gm321* alleles were likely to be strong loss-of-function or null alleles, as they displayed similar phenotypes and were not enhanced when in *trans* to the deficiency *eDf2* (Nishiwaki 1999) (data not shown). It was unexpected that the deletion allele *tm2007* was weaker than *k140* and *gm321* especially with regard to the anterior DTC migration. We examined the phenotype of *k140/tm2007* heterozygotes. The phenotypic penetrance of *k140/tm2007* was 60 ± 8% for anterior and 92 ± 5% for posterior (n = 60) compared to those of *k140*, 56 ± 4% for anterior and 88 ± 3% for posterior (n = 60), and for *tm2007*, 27 ± 5% for anterior and 85 ± 7% for posterior (n = 60). Thus, the heterozygotes exhibited the phenotypic penetrance similar to that of *k140*. We speculate that the *tm2007* strain might have a weak recessive suppressor mutation that can weaken the DTC defects of *tm2007*.

mig-18 acts in the same pathway with mig-17 to control directional migration of DTCs

The phenotypic characteristics of the *mig-18* mutants were similar to those of the *mig-17* mutants (Nishiwaki *et al.* 2000). Therefore we generated double mutants between the *mig-17(k174)* null allele (Ihara and Nishiwaki 2007) and *mig-18(k140)*. The phenotypic penetrance of the double mutants was not stronger than that of *mig-17(k174)*, but it was stronger than that of *mig-18* single mutants, especially with respect to effects on anterior DTCs, suggesting that *mig-18* acts in the *mig-17* pathway.

mig-17 encodes a secreted metalloprotease of the ADAMTS family. MIG-17 is produced in the body-wall muscle cells, is

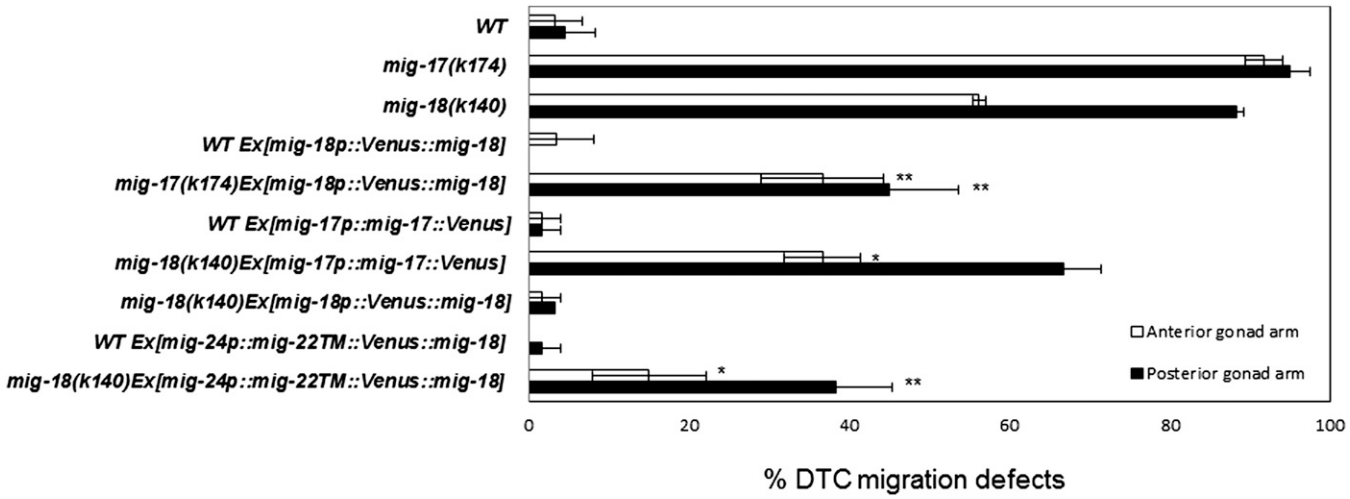

Figure 4 Transgenic rescue of DTC migration defects in *mig-17* and *mig-18* animals. The DTC migration defects of anterior and posterior gonad arms are indicated as percentages. *Ex* indicates an extrachromosomal array. Data are shown as the mean ± SD (n = 60 for each experiment). *P*-values for Fisher's exact test against *mig-17(k174)* for *mig-17* transgenic strains and against *mig-18(k140)* for *mig-18* transgenic strains are indicated: $^{**}P < 0.01$; $^{*}P < 0.05$.

secreted into the body cavity, and becomes localized to the surface of the gonad (Nishiwaki *et al.* 2000). We examined MIG-17-Venus localization in the *mig-18* mutants. MIG-17-Venus localized to the gonadal basement membrane in the *mig-18* mutants, similar to its localization in wild type (Figure 3A and Figure S2), suggesting that *mig-18* is not required for gonadal localization of MIG-17.

MIG-17 is secreted as a proform, with the prodomain present at its N terminus. This pro-MIG-17 is recruited to the gonadal basement membrane in the prodomain-dependent manner (prodomain targeting) (Ihara and Nishiwaki 2007), where it becomes its mature, active form by proteolytic removal of the prodomain, which is catalyzed by its auto-catalytic activity. Mature MIG-17 then participates in controlling the directed migration of DTCs (Ihara and Nishiwaki 2007). To understand whether MIG-18 functions in the activation of MIG-17, we performed Western blot analysis of MIG-17-GFP. We found that the intensities of the bands for the mature form relative to those of the proform were 0.82 and 0.78 for the wild-type and the *mig-18(k140)* mutant animals, respectively (Figure 3B). These results suggest that the processing of the prodomain occurred normally in *mig-18* mutants and that MIG-18 is not required for this process.

To determine the tissue distribution of MIG-18, we generated MIG-18-Venus, a C-terminal fusion construct. This construct, however, was not functional as it failed to rescue the *mig-18* mutant phenotype (data not shown). Thus, we generated a *signal peptide (SP)*::*Venus*::*mig-18* N-terminal fusion construct that is driven by the *mig-18* promoter (*mig-18p*::*SP*::*Venus*::*mig-18*). Venus-MIG-18 rescued the defective DTC migration in the *mig-18* mutants, indicating that the fusion protein is functional (Figure 4). We found that Venus-MIG-18 was expressed in the body-wall muscle cells and the gonadal basement membrane (Figure 3C). Venus-MIG-18 is secreted from the muscle cells because it accumulated in the cytoplasm of the muscle cells and failed to localize to the gonadal basement membrane when its signal peptide was deleted (*mig-18p*:: *ΔSP*::*Venus*::*mig-18*; Figure S3). Thus MIG-18 and MIG-17 proteins are produced and delivered in the same manner. We asked whether the gonadal localization of Venus-MIG-18 requires MIG-17 activity. Venus-MIG-18 localization was not affected in the *mig-17* mutants (Figure 3C and Figure S2), indicating that MIG-17 is not required for gonadal localization of MIG-18.

We examined whether MIG-18 and MIG-17 colocalize in the gonadal basement membrane. Co-expression of Venus-MIG-18 and MIG-17-mCherry revealed clear colocalization of these proteins in the gonadal basement membrane (Figure 3D).

mig-18 and mig-17 act cooperatively to control DTC migration

Because the transgenic extrachromosomal arrays containing MIG-17-Venus and Venus-MIG-18 are expected to contain multiple copies of these constructs, it is likely that their respective genes are overexpressed as compared with the endogenous genes. We examined whether overexpression of MIG-17-Venus in the *mig-18* mutants and whether overexpression of Venus-MIG-18 in the *mig-17* mutants could suppress the defective DTC migration of these mutants. Interestingly, we observed partial rescue in both of these experiments (Figure 4). These results suggest that MIG-18 and MIG-17 do not function sequentially but instead act cooperatively to control DTC migration.

The MIG-17-TM-Venus construct can suppress the DTC migration defects of *mig-17* mutants when it is expressed in the DTC cell membrane (Ihara and Nishiwaki 2007). Using the type II transmembrane domain of MIG-22 (Suzuki *et al.* 2006), we generated *mig-24p*::*mig-22TM*::*Venus*::*mig-18* and expressed it under the control of the DTC-specific *mig-24* promoter (Tamai and Nishiwaki 2007). This membrane-bound

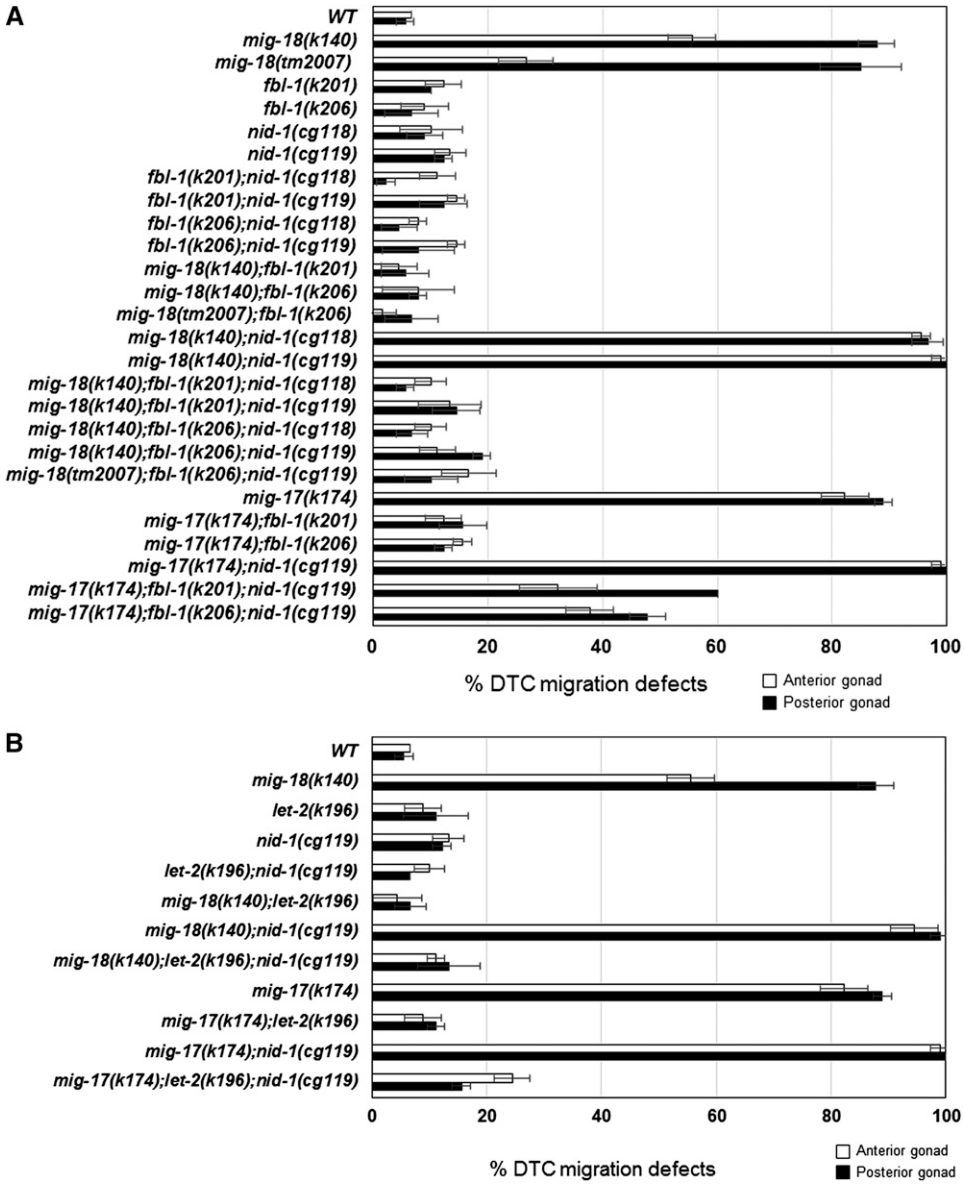

Figure 5 Suppression of *mig-18* and *mig-17* by *fbl-1* and *let-2* mutations. The DTC migration defects of anterior and posterior gonad arms are indicated as percentages. (A) Suppression by *fbl-1 (k201)* and *fbl-1(k206)* alleles. (B) Suppression by the *let-2(k196)* allele. Data are shown as the mean ± SD (n = 60 for each experiment).

construct partially but significantly rescued the DTC migration defects of *mig-18(k140)* mutant animals (Figure 4). The fluorescence in these animals was detected exclusively in the DTCs (Figure S4). MIG-18 activity at the DTC surface may not be sufficient for its full effect on controlling DTC migration. Alternatively, native MIG-18 activity may be sufficient when it is localized to the DTC surface, but the membrane anchoring of this construct could partially perturb its activity. The observation that *mig-18* acts in the same pathway with *mig-17*, whose function is sufficient at the DTC surface (Ihara and Nishiwaki 2007), supports the latter possibility.

Genetic suppressors of mig-17 also suppress mig-18

We previously reported that amino acid substitutions in the basement membrane proteins fibulin-1/FBL-1 and the α2 subunit of collagen IV/LET-2 act as dominant gain-of-function suppressors of *mig-17* mutants (Kubota *et al.* 2004, 2008). The suppressor *fbl-1(gf)* mutants act in a *nid-1*-dependent manner, whereas the suppressor *let-2(gf)* mutants act independently of *nid-1* (Kubota *et al.* 2008). If *mig-18* acts in the same pathway with *mig-17*, it is possible that the suppressor mutations *fbl-1(gf)* and *let-2(gf)* could suppress *mig-18* mutants as well. As expected, the *gf* mutations *fbl-1(k201)*, *fbl-1(k206)*, and *let-2(k196)* all suppressed the DTC migration defects of *mig-18(k140)* mutants (Figure 5, A and B). We introduced *nid-1(cg119)*, a null allele, and *nid-1(cg118)*, a hypomorphic allele that lacks the G2 domain, into *mig-18 (k140)* (Kang and Kramer 2000). Although DTC migration was mostly normal in these *nid-1* single mutants, they enhanced the DTC phenotype of *mig-18(k140)* mutants; a similar enhancement was seen in *mig-17(k174)* mutants (Figure 5A). *let-2(k196)* suppressed *mig-18(k140)* in the *nid-1 (cg119)* mutant background, indicating that the suppression is *nid-1* independent, as was observed for the suppression of

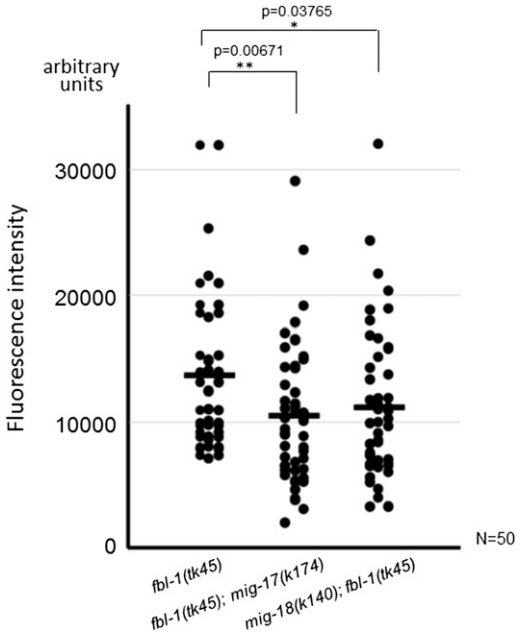

Figure 6 Gonadal localization of FBL-1C-Venus in *mig-17* and *mig-18* mutants. Levels of accumulation of FBL-1C-Venus in the gonadal basement membrane were quantified with confocal microscopy. The fluorescence intensity is given in arbitrary units. Strains are *fbl-1(tk45)*, *mig-17(k174)*; *fbl-1(tk45)* [which contains *unc-42(e270)*], and *mig-18(k140)*; *fbl-1(tk45)*, each of which expressed *fbl-1C*::*Venus*. Each dot represents the fluorescence intensity of a single animal. The horizontal bars represent mean values. *P*-values for Fisher's exact test against *fbl-1(tk45)* are indicated.

mig-17 (Figure 5B). Interestingly, however, the suppression activities of *fbl-1(k201)* and *fbl-1(k206)* mutants did not depend on *nid-1*, as they did in the *mig-17* mutants (Figure 5A). These observations and the more severe DTC phenotypes of the *mig-17* mutants compared to *mig-18* mutants suggest that, although MIG-18 and MIG-17 act in the same pathway, MIG-17 could have some functions that are not shared with MIG-18.

Both MIG-18 and MIG-17 function in FBL-1C accumulation in the gonadal basement membrane

MIG-17 is required for efficient accumulation of FBL-1C/fibulin-1C in the basement membrane (Kubota *et al.* 2004). Using confocal microscopy, we quantified the levels of FBL-1C-Venus that localized to the gonadal basement membrane. We observed that they were significantly lower in both *mig-17* and *mig-18* mutants as compared with the amounts observed in the wild type (Figure 6). These results suggest that not only *mig-17* but also *mig-18* participate in the efficient accumulation of FBL-1C in the gonadal basement membrane.

In *mig-17* mutants, the localization of NID-1 in the basement membrane is also reduced, and the overexpression of NID-1 can partially rescue the DTC migration defects (Kubota *et al.* 2008). We found that overexpression of NID-1 also partially rescued the *mig-18(k140)* mutant and that this effect of NID-1 overexpression was weakened in the *nid-1(cg119)* null mutant background (Figure 7), suggesting that NID-1 accumulation also plays a role downstream of MIG-18.

Discussion

In this study, we identified a novel molecule, MIG-18, that is required for the directional control of DTC migration. We found that MIG-18 acts in the MIG-17 pathway, which we characterized previously as being required for DTC migration (Kubota *et al.* 2008). Although the substrate for MIG-17 is still unclear, MIG-17-dependent proteolysis is required for efficient accumulation of FBL-1C in the gonadal basement membrane. FBL-1C and LET-2 are likely to be activated in the basement membrane by MIG-17 activity, and their activation in turn recruits NID-1 to induce proper DTC migration (Kubota *et al.* 2008). Because we observed the partial rescue of DTC migration defects both when MIG-18 was overexpressed in *mig-17* mutants and when MIG-17 was overexpressed in *mig-18* mutants, we suggest that MIG-18 acts

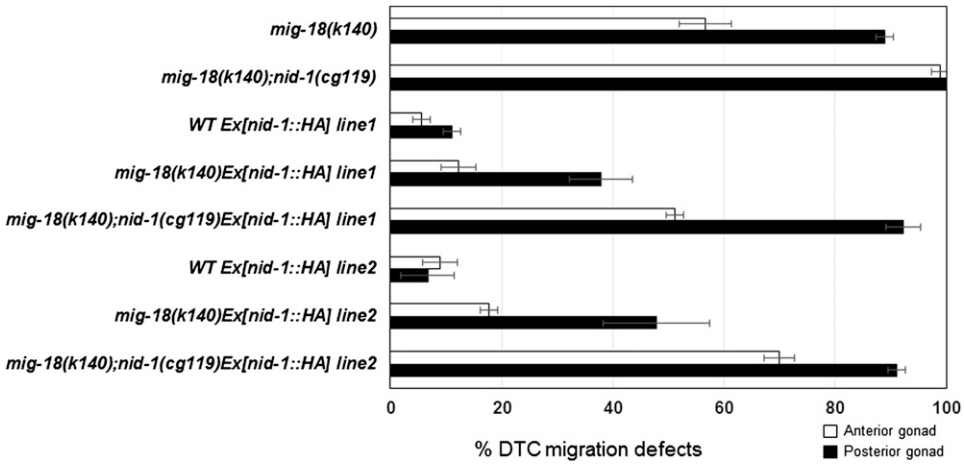

Figure 7 Suppression of *mig-18* by overexpression of NID-1-HA. The DTC migration defects of anterior and posterior gonad arms are indicated as percentages. Lines 1 and 2 have independently generated transgenic extrachromosomal arrays that contain *nid-1*::*HA* corresponding to those reported previously (Kubota *et al.* 2008). Data are shown as the mean ± SD (n = 60 for each experiment).

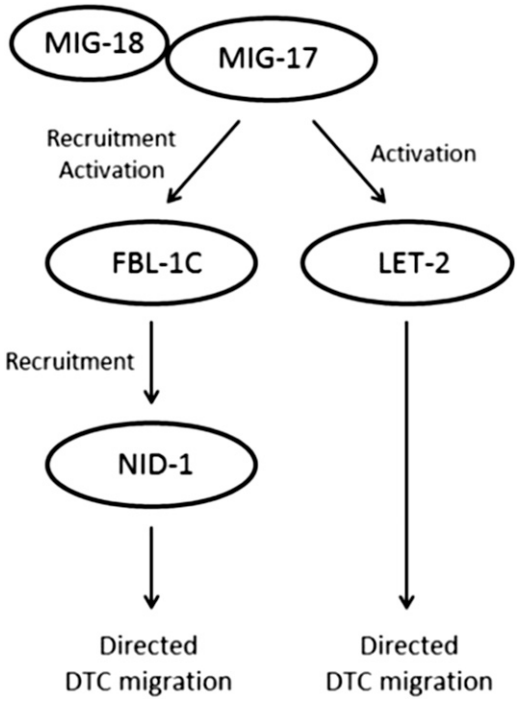

Figure 8 Model of MIG-17- and MIG-18-dependent regulation of DTC migration. MIG-18 acts as a cofactor to activate MIG-17. The activated MIG-17 efficiently recruits FBL-1C to the gonadal basement membrane, where it activates FBL-1C and LET-2. The activated FBL-1C recruits NID-1 to control DTC migration.

cooperatively with MIG-17 rather than upstream or downstream of MIG-17.

It is surprising that overexpression of MIG-18, which appears not to be a protease based on its amino acid sequence, can partially compensate for the loss of the MIG-17 protease in the regulation of DTC migration. One explanation for this might be that MIG-17, when localized to the basement membrane, may also function in DTC migration through its noncatalytic activity by recruiting FBL-1C. This function should, however, be a minor one, as the ability of MIG-17 to control DTC migration strongly depends on its catalytic activity (Ihara and Nishiwaki 2007). Interestingly, there are some reports regarding noncatalytic activities of ADAMTSs. Mammalian ADAMTS10 participates in microfibril biogenesis through its binding to fibrillin-1, in which the catalytic activity of ADAMTS10 appears not to be involved (Kutz *et al.* 2011). ADAMTS4 binds and colocalizes with fibronectin at the cell surface, where fibronectin can inhibit ADAMTS4 activity as an aggrecanase (Hashimoto *et al.* 2004). In addition, the *Xenopus* ADAMTS1 negatively modulates FGF signaling independently of its metalloprotease activity (Suga *et al.* 2006).

Because MIG-18 and MIG-17 act in the same pathway, we expected that the suppression of *mig-18* mutants by the *fbl-1* and *let-2* gain-of-function mutations would be dependent and independent of *nid-1*, respectively. However, the *fbl-1* mutations suppressed *mig-18* in a *nid-1*-independent manner. This result is different from the suppression of *mig-17* mutants by *fbl-1(gf)*, which is dependent on *nid-1* (Kubota *et al.* 2008). However, because the *nid-1* dependency of *mig-17* suppression was partial (Figure 5A), it is possible that NID-1 may not be a critical component of the MIG-17 pathway for controlling DTC migration. We propose a model in which MIG-18 is a cofactor that enhances the catalytic and noncatalytic activities of mature (*i.e.*, after removal of the prodomain) MIG-17. MIG-18-enhanced MIG-17 recruits FBL-1C efficiently to the gonadal basement membrane and activates FBL-1C and LET-2. The activated FBL-1C recruits NID-1 to the gonadal basement membrane (Figure 8). Because the phenotype of *mig-17* mutants is stronger than that of *mig-18* mutants, we postulated in this model that MIG-17 has a basal activity even in the absence of MIG-18. In the *mig-17(k174)*; *fbl-1(gf)* double mutants, the FBL-1C mutant protein weakly localizes to the gonadal basement membrane (Kubota *et al.* 2004), but it is not activated at all by MIG-17. Thus, the FBL-1C mutant protein requires NID-1 to regulate DTC migration. In contrast, in the *mig-18(k140)*; *fbl-1(gf)* double mutants, the basal activity of MIG-17 activates the FBL-1C mutant protein, and therefore NID-1 is dispensable in DTC regulation. Although it is not clear why the *mig-18* mutation (and also the *mig-17* mutation) was partially suppressed by the overexpression of *nid-1*, it is possible that with overexpression more NID-1 molecules were able to localize to the basement membrane of *mig-18* and *mig-17* mutants even though FBL-1C was not fully activated.

MIG-18 appears to be a novel protein, but it has partial homologies to CCN proteins found in mammals. Proteins in the CCN family are known as matricellular proteins, which have been defined as a subset of nonstructural proteins in the extracellular matrix that can modulate cell-matrix interactions and cell regulatory functions by different mechanisms (Roberts 2011). In this respect, MIG-18 should also be classified as a matricellular protein. The CCN proteins are involved in the regulation of various cellular functions, such as proliferation, differentiation, survival, adhesion, and migration (Leask and Abraham 2006). CCN6 is highly upregulated in osteoarthritic cartilage and is suggested to act in progressive pseudorheumatoid dysplasia through transcriptional repression of ADAMTS-5 and expression of MMP-10 (Baker *et al.* 2012). CCN3 is not expressed in advanced melanoma cells, and its expression in aggressive Lu melanoma cells inhibits MMP-2/9 transcription and results in reduced tumor invasion (Fukunaga-Kalabis *et al.* 2008). CCN3 enhances the migration of chondrosarcoma cells by increasing expression of MMP-13 through integrin receptors (Tzeng *et al.* 2011). Therefore CCN proteins are involved in the transcriptional regulation of matrix metalloproteinases. However, the functions of CCN proteins in post-translational control of matrix metalloproteinases remain to be determined. Our findings suggest that matricellular proteins may be involved in the post-translational regulation of activities of ADAMTS proteinases during development and during disease pathology.

Acknowledgments

We thank Shigehiro Kuraku (RIKEN Center for Developmental Biology) and Hiroki Kaneko (College of Humanities and Sciences, Nihon University) for helpful discussions and Noriko Nakagawa and Asami Sumitani for technical assistance. Some nematode strains used in this work were provided by the Caenorhabditis Genetics Center, which is funded by the National Institutes of Health National Center for Research Resources, and by Shohei Mitani through the National Bioresource Project for the nematode. This work was supported by a Grant-in-Aid for Scientific Research on Innovative Areas by the Ministry of Education, Culture, Sports, Science and Technology (K.N.) (22111005) and by National Institutes of Health grant NS32057 (G.G.).

Literature Cited

Apte, S. S., 2009 A disintegrin-like and metalloprotease (reprolysin-type) with thrombospondin type 1 motif (ADAMTS) superfamily: functions and mechanisms. J. Biol. Chem. 284: 31493–31497.

Baker, N., P. Sharpe, K. Culley, M. Otero, D. Bevan *et al.*, 2012 Dual regulation of metalloproteinase expression in chondrocytes by Wnt-1-inducible signaling pathway protein 3/CCN6. Arthritis Rheum. 64: 2289–2299.

Blelloch, R., and J. Kimble, 1999 Control of organ shape by a secreted metalloprotease in the nematode *Caenorhabditis elegans*. Nature 399: 586–590.

Brenner, S., 1974 The genetics of *Caenorhabditis elegans*. Genetics 77: 71–94.

Chen, C. C., and L. F. Lau, 2009 Functions and mechanisms of action of CCN matricellular proteins. Int. J. Biochem. Cell Biol. 41: 771–783.

Chen, N., S. J. Leu, V. Todorovic, S. C. Lam, and L. F. Lau, 2004 Identification of a novel integrin alphavbeta3 binding site in CCN1 (CYR61) critical for pro-angiogenic activities in vascular endothelial cells. J. Biol. Chem. 279: 44166–44176.

De Stasio, E. A., and S. Dorman, 2001 Optimization of ENU mutagenesis of *Caenorhabditis elegans*. Mutat. Res. 495: 81–88.

Enomoto, H., C. M. Nelson, R. P. Somerville, K. Mielke, L. J. Dixon *et al.*, 2010 Cooperation of two ADAMTS metalloproteases in closure of the mouse palate identifies a requirement for versican proteolysis in regulating palatal mesenchyme proliferation. Development 137: 4029–4038.

Fukunaga-Kalabis, M., G. Martinez, S. M. Telson, Z. J. Liu, K. Balint *et al.*, 2008 Downregulation of CCN3 expression as a potential mechanism for melanoma progression. Oncogene 27: 2552–2560.

Hashimoto, G., M. Shimoda, and Y. Okada, 2004 ADAMTS4 (aggrecanase-1) interaction with the C-terminal domain of fibronectin inhibits proteolysis of aggrecan. J. Biol. Chem. 279: 32483–32491.

Hedgecock, E. M., J. G. Culotti, D. H. Hall, and B. D. Stern, 1987 Genetics of cell and axon migrations in *Caenorhabditis elegans*. Development 100: 365–382.

Ihara, S., and K. Nishiwaki, 2007 Prodomain-dependent tissue targeting of an ADAMTS protease controls cell migration in *Caenorhabditis elegans*. EMBO J. 26: 2607–2620.

Kang, S. H., and J. M. Kramer, 2000 Nidogen is nonessential and not required for normal type IV collagen localization in *Caenorhabditis elegans*. Mol. Biol. Cell 11: 3911–3923.

Kubota, Y., R. Kuroki, and K. Nishiwaki, 2004 A fibulin-1 homolog interacts with an ADAM protease that controls cell migration in *C. elegans*. Curr. Biol. 14: 2011–2018.

Kubota, Y., K. Ohkura, K. K. Tamai, K. Nagata, and K. Nishiwaki, 2008 MIG-17/ADAMTS controls cell migration by recruiting nidogen to the basement membrane in *C. elegans*. Proc. Natl. Acad. Sci. USA 105: 20804–20809.

Kutz, W. E., L. W. Wang, H. L. Bader, A. K. Majors, K. Iwata *et al.*, 2011 ADAMTS10 protein interacts with fibrillin-1 and promotes its deposition in extracellular matrix of cultured fibroblasts. J. Biol. Chem. 286: 17156–17167.

Leask, A., and D. J. Abraham, 2006 All in the CCN family: essential matricellular signaling modulators emerge from the bunker. J. Cell Sci. 119: 4803–4810.

Maduro, M., and D. Pilgrim, 1995 Identification and cloning of *unc-119*, a gene expressed in the *Caenorhabditis elegans* nervous system. Genetics 141: 977–988.

McCulloch, D. R., C. M. Nelson, L. J. Dixon, D. L. Silver, J. D. Wylie *et al.*, 2009 ADAMTS metalloproteases generate active versican fragments that regulate interdigital web regression. Dev. Cell 17: 687–698.

Mello, C. C., J. M. Kramer, D. Stinchcomb, and V. Ambros, 1991 Efficient gene transfer in *C.elegans*: extrachromosomal maintenance and integration of transforming sequences. EMBO J. 10: 3959–3970.

Nishiwaki, K., 1999 Mutations affecting symmetrical migration of distal tip cells in *Caenorhabditis elegans*. Genetics 152: 985–997.

Nishiwaki, K., N. Hisamoto, and K. Matsumoto, 2000 A metalloprotease disintegrin that controls cell migration in *Caenorhabditis elegans*. Science 288: 2205–2208.

Roberts, D. D., 2011 Emerging functions of matricellular proteins. Cell. Mol. Life Sci. 68: 3133–3136.

Stupka, N., C. Kintakas, J. D. White, F. W. Fraser, M. Hanciu *et al.*, 2013 Versican processing by a disintegrin-like and metalloproteinase domain with thrombospondin-1 repeats proteinases-5 and -15 facilitates myoblast fusion. J. Biol. Chem. 288: 1907–1917.

Suga, A., H. Hikasa, and M. Taira, 2006 *Xenopus* ADAMTS1 negatively modulates FGF signaling independent of its metalloprotease activity. Dev. Biol. 295: 26–39.

Suzuki, N., H. Toyoda, M. Sano, and K. Nishiwaki, 2006 Chondroitin acts in the guidance of gonadal distal tip cells in *C. elegans*. Dev. Biol. 300: 635–646.

Tamai, K. K., and K. Nishiwaki, 2007 bHLH transcription factors regulate organ morphogenesis via activation of an ADAMTS protease in *C. elegans*. Dev. Biol. 308: 562–571.

Tzeng, H. E., J. C. Chen, C. H. Tsai, C. C. Kuo, H. C. Hsu *et al.*, 2011 CCN3 increases cell motility and MMP-13 expression in human chondrosarcoma through integrin-dependent pathway. J. Cell. Physiol. 226: 3181–3189.

Wicks, S. R., R. T. Yeh, W. R. Gish, R. H. Waterston, and R. H. Plasterk, 2001 Rapid gene mapping in *Caenorhabditis elegans* using a high density polymorphism map. Nat. Genet. 28: 160–164.

Communicating editor: M. Sundaram

GENETICS

Supporting Information
http://www.genetics.org/lookup/suppl/doi:10.1534/genetics.113.157685/-/DC1

The Novel Secreted Factor MIG-18 Acts with MIG-17/ADAMTS to Control Cell Migration in *Caenorhabditis elegans*

Hon-Song Kim, Yuko Kitano, Masataka Mori, Tomomi Takano, Thomas Edward Harbaugh, Kae Mizutani, Haruka Yanagimoto, Sayaka Miwa, Shinji Ihara, Yukihiko Kubota, Yukimasa Shibata, Kohji Ikenishi, Gian Garriga, and Kiyoji Nishiwaki

DOI: 10.1534/genetics.113.157685

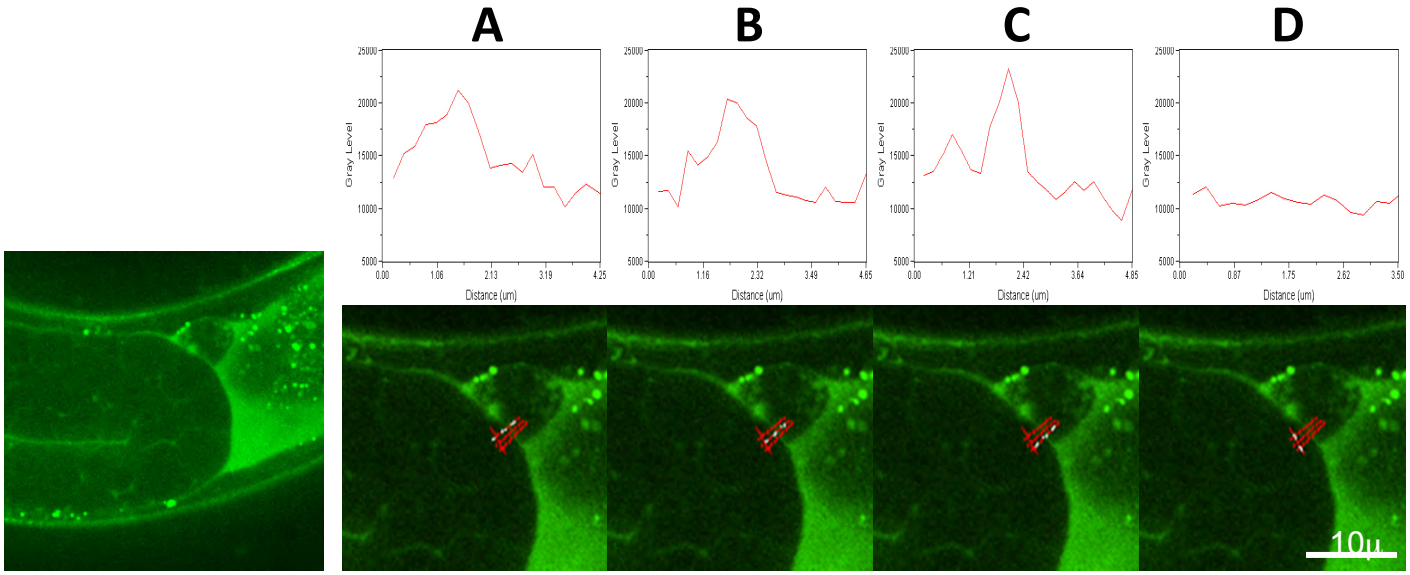

Figure S1 Quantitative analysis of FBL-1C-Venus. Sample data for *fbl-1(tk45) Ex[fbl-1C::Venus]* are shown. For each sample, confocal images of the sagittal section of the gonads were obtained with a Zeiss Imager M2 microscope equipped with a spinning-disk confocal scan head (CSU-X1; Yokogawa) and an ImageEM CCD camera (ImageEM; Hamamatsu Photonics). Using ImageJ software, fluorescence intensities along three drawn lines, each of which crossed the basement membrane (A to C), were measured; the average background intensities inside the gonad (D) were subtracted from the peak values, and the resulting corrected values were averaged.

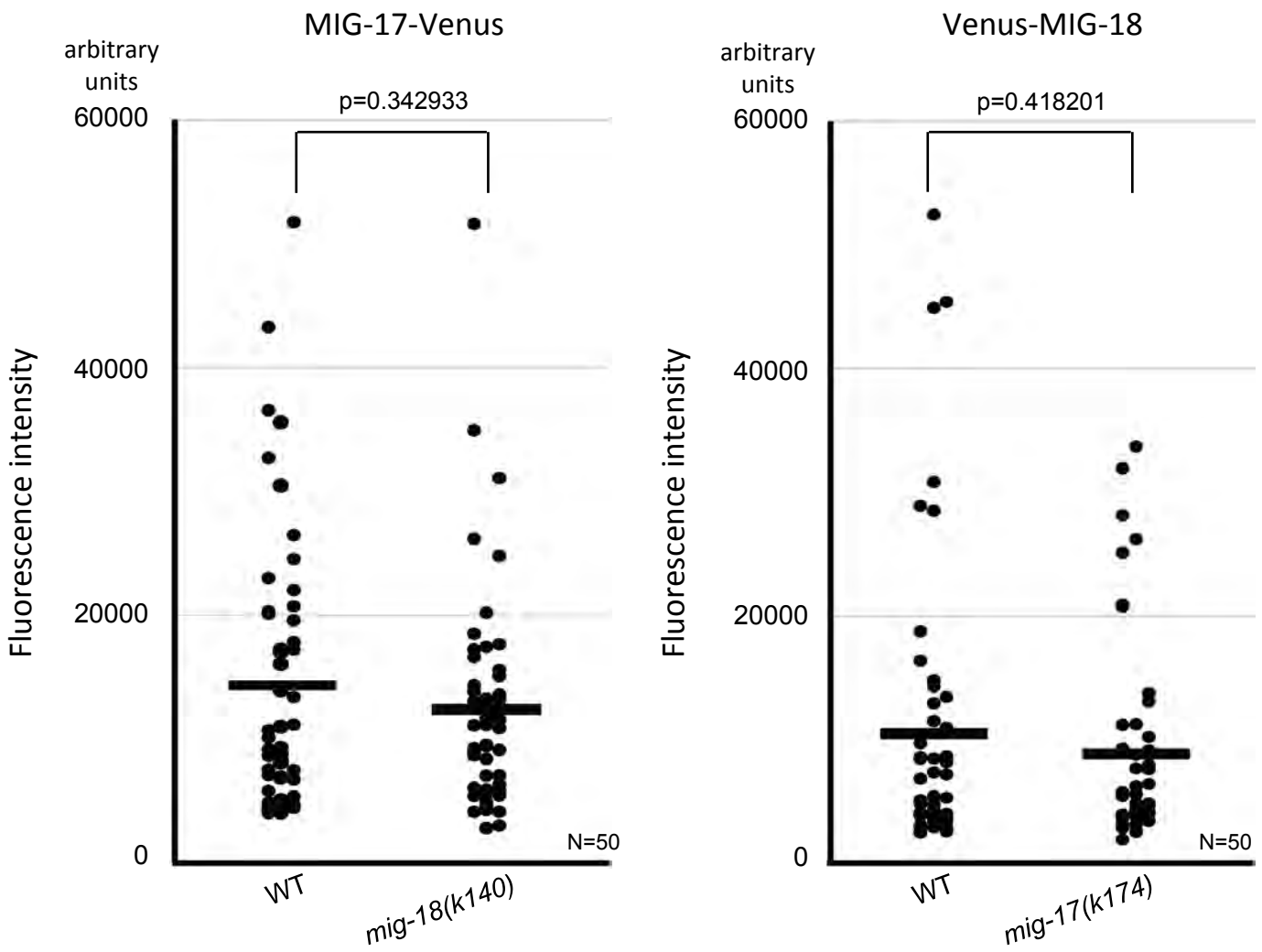

Figure S2 Quantification of gonadal localization of MIG-17-Venus and Venus-MIG-18. The strains in Figure 3A and C were used. Fluorescence intensities of gonadal basement membrane were analyzed with similar procedures as described in Figure S1. The vertical scale is given in arbitrary units. Each dot represents the fluorescence intensity of a single animal. The horizontal bars represent mean values. *P*-values for Fisher's exact test against WT are indicated.

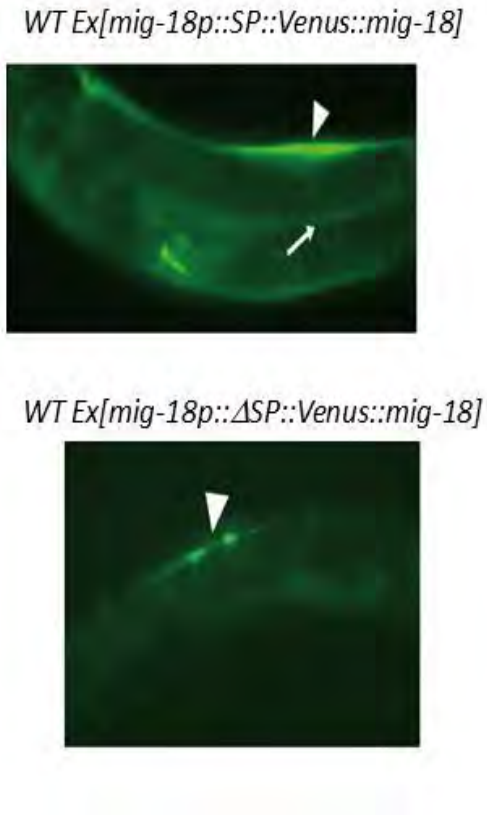

Figure S3 Expression of *mig-18p::ΔSP::Venus::mig-18*. A wild-type animal expressing *mig-18p::Venus::mig-18* (upper) exhibited fluorescent signals in both the body wall muscles (arrowhead) and the surface of the gonad (arrow). The wild-type animal expressing *mig-18p:: ΔSP::Venus::mig-18* (lower) exhibited signals only in the body wall muscles (arrowhead).

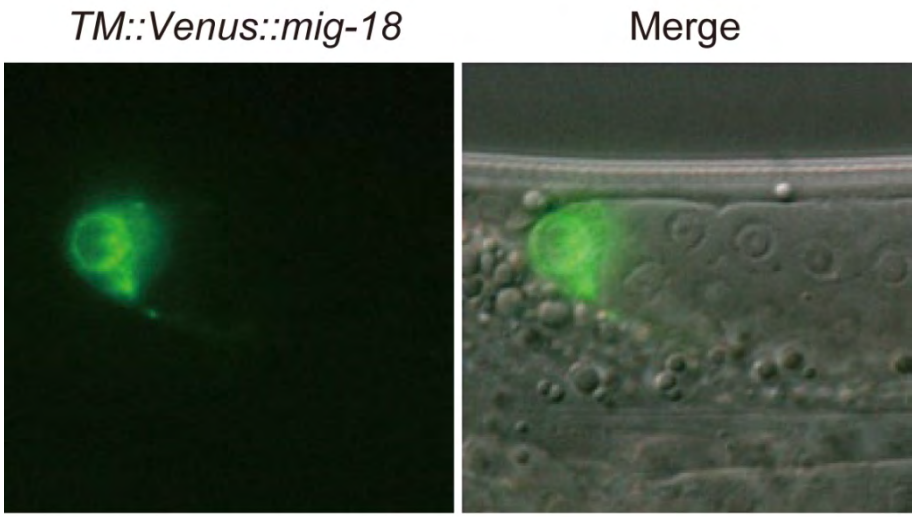

Figure S4 Expression of *mig-24p::TM::Venus::mig-18*. Fluorescence (left) and merged fluorescence and Nomarski (right) images of a DTC in a young-adult hermaphrodite expressing *mig-24p::TM::Venus::mig-18* is shown.